Available online at www.scholarsresearchlibrary.com

Scholars Research Library

Archives of Physics Research, 2011, 2 (1): 107-126
(http://scholarsresearchlibrary.com/archive.html)

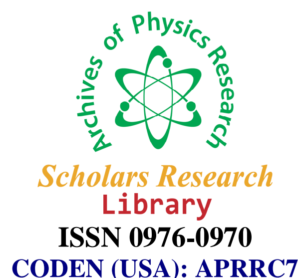

ISSN 0976-0970
CODEN (USA): APRRC7

Heat Sink Design for IMPATT Diode Sources with Different Base Materials Operating at 94 GHz

[1]Aritra Acharyya, [2]Jayanta Mukherjee, [3]Moumita Mukherjee and [4]J. P. Banerjee

[1,4]Institute of Radio Physics and Electronics, University of Calcutta, Kolkata, India
[2]Department of Physics, Rabindra Mahavidyalaya, Hooghly, WB, India
[3]CMSDS, Institute of Radio Physics and Electronics, University of Calcutta, Kolkata, India

---

ABSTRACT

A very useful method of formulating the Total Thermal Resistance of ordinary mesa structure of DDR IMPATT diode oscillators are presented in this paper. Calculation of Total Thermal Resistance of the device along with other components associated with it, maintaining acceptable accuracy is very much important to determine the thermal performance of the oscillator during continuous wave steady state operation. A lumped analytical model of heat transfer in ordinary mesa structure of DDR IMPATT diode on semi-infinite heat sink is developed, from which the entire thermal resistance formulation is done. Calculations of Total thermal resistances associated with different DDR IMPATT diodes with different base materials operating at 94 GHz (W-Band) are included in this paper using the author's developed formulation for both type-IIA diamond and copper semi-infinite heat sinks separately. Heat Sinks are designed using both type-IIA diamond and copper for all those diodes to operate near 500 K (which is well below the burn-out temperatures of all those base materials) for CW steady state operation. Mathematical expression of temperature inside the heat sink as a function of radius and thickness is developed and using this expression the temperature profiles inside the heat sinks are investigated thoroughly. Results are provided in the form of necessary plots and tables. This formulation will be very useful tool to design Heat sinks for practical IMPATT oscillators.

Keywords: Heat Sink, IMPATT Diode, Junction Temperature, Lumped Analytical Model, Ordinary Mesa Structure, Thermal Resistance.

INTRODUCTION

The recent advances in IMPATT device technology has made it possible to use this device in various communication systems operating in millimeter wave and sub-millimeter wave bands of frequency ranges which provides advantages such as increased resolution and use of low voltage

power supplies. The availability of several atmospheric window frequencies in the mm-wave frequency range (30-300 GHz) has further increased the usefulness of IMPATT diodes which can now produce appreciable amounts of millimeter wave power at very high frequencies of operation. Last four decades, several workers have been exploring the possibility of high-power generation either from a single IMPATT diode or from the several diodes by using power combining techniques. It is well known that the efficiency of the IMPATT diode is relatively low [Practically 5-15% for CW operation], a large fraction of the dc power is dissipated as heat in the high-field region. The temperature of the junction rises above ambient, and in many cases output power of oscillator is limited by the rate at which heat can be extracted from the device. As junction temperature increases, the reverse saturation current rises exponentially and eventually leads to *thermal runway phenomenon* resulting the burning out of the device. Since in contrast to the avalanche current, the reverse saturation current does not require a large voltage to sustain it, the voltage begins to decrease when the junction gets hot enough for the reverse current to constitute a significant fraction of the total current. A thermally induced DC negative resistance is produced, causing the current to concentrate in the hottest part of the diode. As well as leading to the eventual burn-out of the junction, the increased saturation current at elevated temperatures produces degradation in the oscillator performance at power levels below the burn-out value. The increased reverse saturation current produces a faster build-up of the avalanche current and degrades the negative resistance of the device. Thus, in general, the oscillator efficiency will begin to decrease at power levels just below the burn-out power. As the band-gap of the semiconductor becomes larger the reverse saturation current associated with it becomes smaller and consequently the burn-out temperature of the junction rises. Thus Ge-IMPATTs ($E_g = 0.7$ eV) are lower power devices than either Si ($E_g = 1.12\ eV$) or GaAs ($E_g = 1.43\ eV$) devices. The amount of DC power, P_{max}, that can be dissipated in a diode is determined by the burn-out temperature T_B and thermal resistance, R_{th}: $P_{max} = (T_B - T_0)/R_{th}$, where, R_{th} is defined as the temperature rise produced at the junction by the dissipation of one Watt of power. Properly designed diode and heat-sink are required for generating appreciable RF power from the CW Si-IMPATT oscillators without device burn-out during steady state operation.

Authors are formulated the total thermal resistance for the actual mesa structure of IMPATT diode oscillator (Figure 1). A lumped analytical model of heat transfer in ordinary mesa structure of DDR IMPATT diode on semi-infinite heat sink is used to determine the total thermal resistance of the whole system that responsible for transferring heat from the p-n junction of the device (Heat Source) to the ambient ($T_0 = 300\ K$). As discussed earlier, due to very small DC to RF conversion efficiency of the CW IMPATT devices a large amount of the DC power actually dissipated in the device during steady state operation of the oscillator. That actually increases its internal temperature (junction temperature) well above the ambient temperature. If the device junction temperature becomes too high, the device may suffer permanent damage or burn-out. That is why IMPATT devices are packaged with heat sinks so that heat can be conducted away from the device during steady state operation. Heat sink dimensions are chosen properly such that total thermal resistance attains such a value that can keep the junction temperature of the device well below the burn-out temperature (different for different base materials) during CW steady state operation of the oscillator.

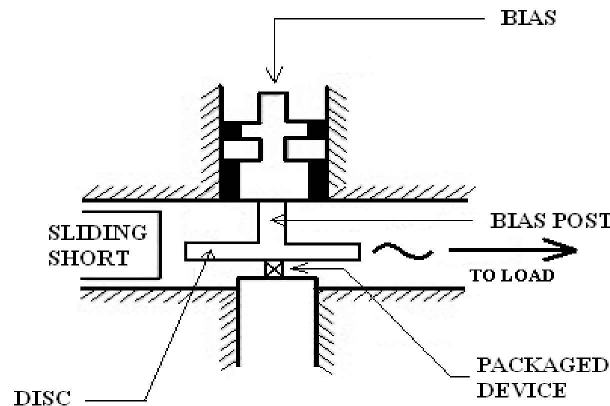

Figure 1: Schematic diagram of W-Band resonant cap cavity.

Schematic diagram of a resonant cap cavity IMPATT oscillator is shown in Figure 1. Heat sink is attached below the device. At the upper side of the device a bias post [Figure 1] is connected with the device through package cap and one or more gold plate lead(s) [Figure 2] to supply DC bias current. So if we consider the junction of the device as the heat source during steady state operation of the oscillator then it is clearly visible that there are two paths for heat from the junction to flow towards the ambient. First one is below the junction, i.e. junction → diode portion below the junction → heat sink → ambient. And the second path is above the junction, i.e. junction → diode portion above the junction → gold plat lead(s) → package cap → disc cap & bias post → ambient. Cut way of packaged IMPATT diode is shown in Figure 2. In this figure the detail structure of the device with the package and heat sink is clearly visible.

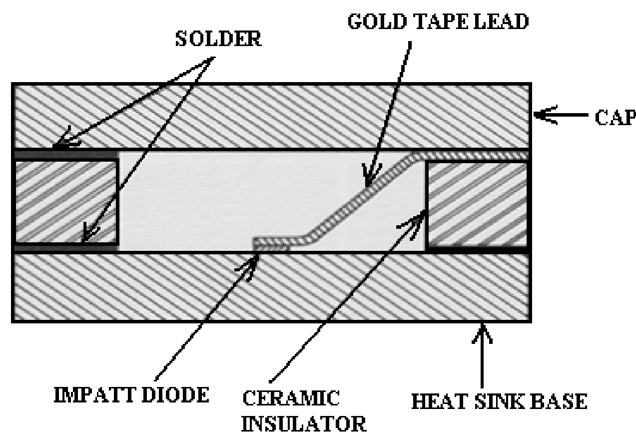

Figure 2: Cut way of Packaged IMPATT Diode.

The rest of this paper is organized as follows. Section II describes the details of the actual formulation of the Total Thermal Resistance. Section III provides the algorithm used to design the heat sinks for IMPATT oscillators to operate in a particular junction temperature during continuous wave steady state operation. Detailed mathematical expression for two-dimensional

temperature distribution inside the heat sink is developed in Section IV. Designed Heat Sink Dimensions (using Diamond and Copper both), calculated Total Thermal Resistances and Junction Temperatures for different CW DDR IMPATT diodes with different base materials operating at 94 GHz (W-Band) are studied and compared in Section V. Results are provided in this section in terms of necessary plots and tables. Temperature distribution inside the heat sinks are found out and presented as graphical form. Finally the paper concludes in Section VI.

1. Formulation of Total Thermal Resistance

Consider a cylindrical block of a material of face area A, thickness L and the temperature of the upper and lower faces are T_1 and T_2 K respectively ($T_1 > T_2$). So heat will conduct from the hotter face to the colder face. If Q be the amount of heat conducted in time t second, then it is found that,

$$Q \propto A$$
$$\propto (T_1 - T_2)$$
$$\propto t$$
$$\propto \frac{1}{L}$$
$$\Rightarrow Q = \frac{kA(T_1 - T_2)t}{L} \quad (1)$$

Where, k is a constant, called *thermal conductivity*.

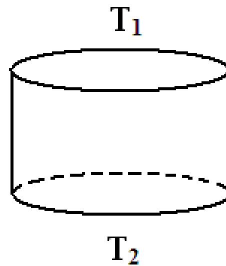

Figure 3: Cylindrical Block.

Now the Thermal Resistance can be defined as,

$$R_{th} = \frac{Temperature\ Change}{Heat\ Flow\ Rate} = \frac{T_1 - T_2}{\left(\frac{Q}{t}\right)} \quad (2)$$

So, the thermal impedance is defined as the temperature rise produced at the junction by the dissipation of one watt of power. Now, using (1) and (2) the thermal resistance of a cylindrical block can be formulated as,

$$R_{th} = \left(\frac{L}{A.k}\right) \quad where,\ A = \pi r^2 \quad [Cylinder\ having\ circular\ cross\ section\ of\ radius\ r] \quad (3)$$

In this paper, our aim is to formulate the Total Thermal Resistance of the packaged IMPATT diode over semi-infinite copper/diamond heat sink. In Figure 4 the actual structure of typical

Silicon based Ordinary Mesa diode over diamond/copper heat sink is shown. The position of the junction along with different layers of the DDR IMPATT diode is shown in this figure in detail. To determine the thermal resistance of the mesa diode, for simplicity its actual structure must be approximated properly without losing accuracy significantly. Three steps of approximation of the different layers of the mesa diode are elaborated in the Figure 5.

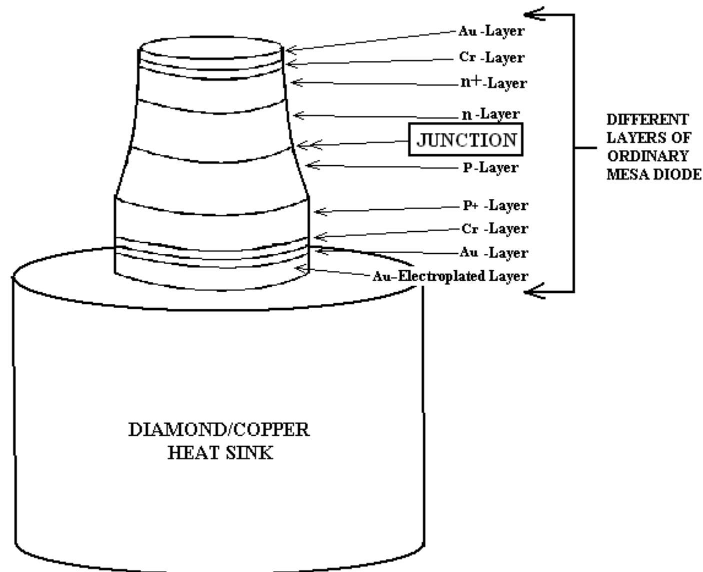

Figure 4: Actual Structures of typical Si based Ordinary Mesa diode over Semi-Infinite Diamond/Copper Heat Sink.

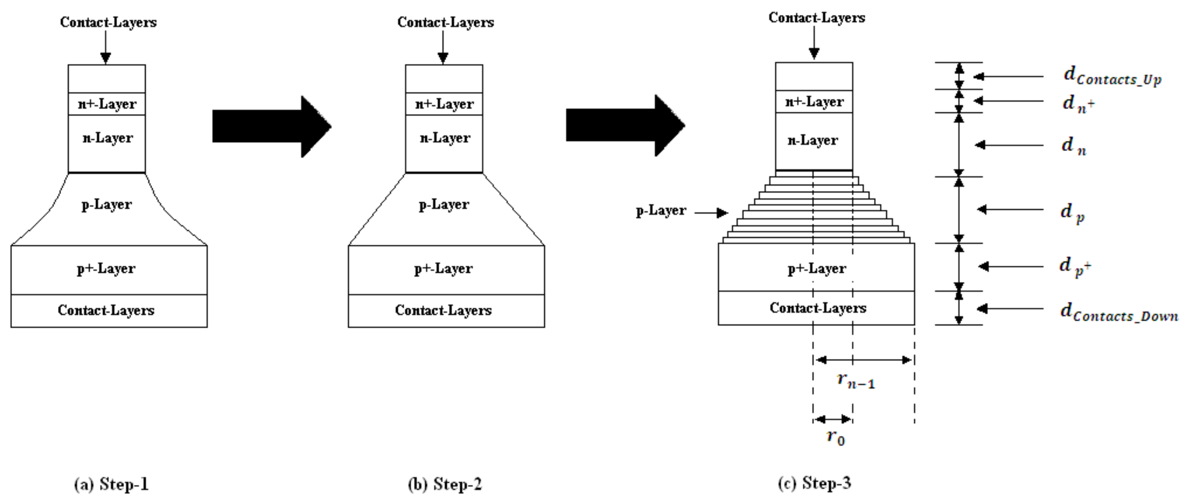

Figure 5: Three Step Approximations for different layers of Ordinary Mesa Structure of DDR IMPATT diode.

In the first step (step-1), different layers are assumed to have the shape described in Figure 5(a). *p*-layer of the mesa DDR diode can be closely approximated to have conical shape (step-2) as shown in Figure 5(b). In the next step (step-3) the *p*-layer of the diode is approximated as n number of concentric cylinders having same axial length (d_p/n) but increasing radius uniformly from r_0 to r_{n-1} (Figure 5(c)). As number of such cylinders (n) increases, the approximation comes

closer to the conical shape. When $n \rightarrow \infty$, then this approximation (step-3) becomes perfectly conical approximation (step-2) of p-layer. Finally p^+ and contact-layers below the junction together are approximated as a cylinder of fixed radius having the radius r_{n-1}. Generally p^+ and contact-layers below the junction have square cross-sections, but in our analysis [for simplicity] these cross-sections are approximated as circular. Heat sinks are also assumed as having circular cross sections. Secondly for the portion of the diode above the junction Silicon n, n^+ and contact-layers above the n^+-layer together are approximated as a cylinder of fixed radius having the radius r_0.

Following the above mentioned assumptions for the diode, now the Total Thermal resistance of the ordinary mesa diode along with the heat sink and other package components and bias-post and disc cap will be formulated in this section. A lumped analytical model of heat transfer in ordinary mesa structure of DDR IMPATT diode on semi-infinite heat sink is shown in Figure 6. Here the p-n junction is considered as the constant heat source (Continuous Wave operation). From the junction of the diode the heat will continuously flow upward [through Diode (above the junction portion), Gold Tape Lead(s), Package Cap, Disc cap & Bias-Post] and downward [through Diode (below the junction portion), Heat Sink] to the ambient during the steady state of operation.

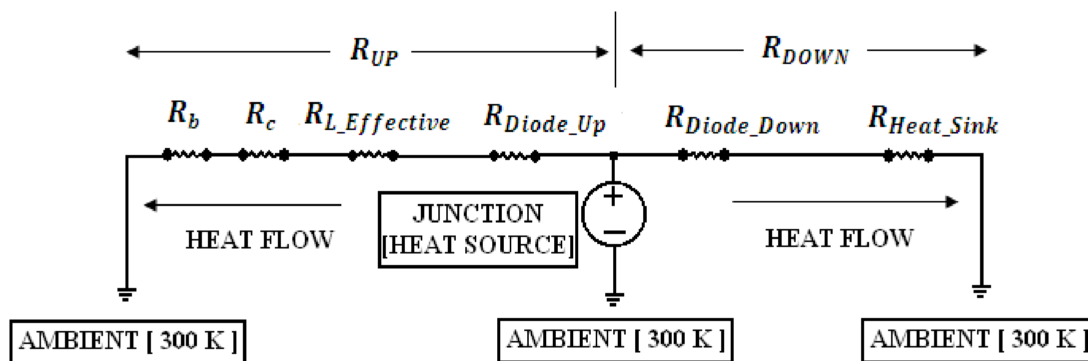

Figure 6: Lumped Analytical Model of Heat Transfer in Ordinary Mesa Structure of DDR IMPATT Diode on Semi-infinite Heat Sink.

First consider the downward portion of the heat flow; the thermal resistance associated with that portion. The thermal resistance of the p-layer of the diode can be formulated as follows,

$$R_p = \frac{1}{\pi} \underset{n\to\infty}{Lt} \sum_{i=0}^{n-1} \left[\frac{\left(\frac{d_p}{n}\right)}{r_i^2 k_{Base_Material}} \right] \quad (2)$$

Where, $(r_{i+1} - r_i) = \frac{(r_{n-1} - r_0)}{(n-1)}$ for, $0 \le i \le (n-2)$. Now the expressions of thermal resistances for p^+-layers is,

$$R_{p^+} = \left[\frac{d_{p^+}}{\pi r_{n-1}^2 k_{Base_Material}} \right] \quad (3)$$

Combined thermal resistance of the contact-layers below the p^+-layer is,

$$R_{Contant_Down} = \frac{1}{\pi}\sum_{i=0}^{m-1}\frac{d_i}{r_{n-1}k_i} \quad (4)$$

Where, d_i and k_i are the thickness and thermal conductivity of the ith contact layer [assuming total m numbers of contact-layers are present]. Therefore the Total Thermal Resistance of the diode below the junction can be written as,

$$R_{Diode_Down} = R_p + R_{p^+} + R_{Contact_Down} \quad (5)$$

Thermal resistance of the Heat Sink will be,

$$R_{Heat_Sink} = \left[\frac{L_H}{\pi R_H^2 k_H}\right] \quad (6)$$

Where, L_H and R_H are the heat sink thickness and radius respectively. So the Total Thermal Resistance below the junction (Diode + Heat Sink) can be expressed as,

$$R_{DOWN} = R_{Diode_Down} + R_{Heat_Sink} \quad (7)$$

Now the Thermal Resistance of the diode above the junction has to be formulated. Following the assumptions in Figure 5 expressions for Thermal Resistances of the n, n^+, and Contact-layers are given below.

$$R_{n\&n^+} = \frac{1}{\pi}\left[\frac{d_n + d_{n^+}}{r_0^2 k_{Base_Material}}\right] \quad (8)$$

Where, d_n and d_{n+} are the thicknesses of the n and n^+-layers respectively. Now the combined thermal resistance of the contact-layers over n^+-layer is,

$$R_{Contant_Up} = \frac{1}{\pi}\sum_{i=0}^{s-1}\frac{d_i}{r_0 k_i} \quad (9)$$

Where, d_i and k_i are the thickness and thermal conductivity of the ith contact layer [assuming total s numbers of contact-layers are present]. Therefore the Total Thermal Resistance of the diode above the junction can be written as,

$$R_{Diode_Up} = R_{n\&n^+} + R_{Contact_Up} \quad (10)$$

The expressions of Thermal resistances of Gold Tape Lead(s), Package Cap and Disc Cap and Bias-post are given in (11), (12) and (13) respectively,

$$R_{L_Effective} = \frac{\left[\dfrac{L_{Lead}}{A_{Effective_Lead}k_{Au}}\right]}{t} \quad (11)$$

Where, t = Number of Lead(s); t = *1* or *2* or *4*.

$$R_c = \left[\frac{L_{package_cap}}{A_{effective_package_cap} k_{Au}}\right] \quad (12)$$

$$R_b = \left[\frac{L_{disc_cap}}{A_{effective_disc_cap} k_{Cu}} + \frac{L_{bias_post}}{A_{effective_bias_post} k_{Cu}}\right] \quad (13)$$

So the Total Thermal Resistance above the junction (Diode + Gold Tape Lead(s) + Package Cap + Disc cap & Bias-post) can be expressed as,

$$R_{UP} = R_{Diode_Up} + R_{L_effective} + R_c + R_b \quad (14)$$

At the steady state heat will flow take place from the junction (source) to the ambient (sink) via two paths. One path is downward the junction and another is upward the junction. Now expressions for the Thermal Resistances for both of these paths are known from equations (1) to (14). From the lumped analytical model of heat transfer in ordinary mesa structure of DDR IMPATT diode on semi-infinite heat sink is shown in Figure 6, it can be concluded that the Equivalent Total Thermal Resistance of the whole system will be the parallel combination of the Thermal Resistances associated with these two paths.

$$R_{TOTAL} = R_{UP} \, // \, R_{DOWN} = \left(\frac{R_{UP} R_{DOWN}}{R_{UP} + R_{DOWN}}\right) = \frac{R_{DOWN}}{1 + \left(\frac{R_{DOWN}}{R_{UP}}\right)} \quad (15)$$

Now the cross-sectional area of a gold tape lead is very small compared to the effective diode cross-sectional area. That is way the effective thermal resistance of gold tape lead(s) [$R_{L_Effective}$] is very large. That makes the value of R_{UP} very much greater compared to R_{DOWN} [$R_{UP} >> R_{DOWN}$]. So, Total Thermal Resistance can be written as,

$$R_{TOTAL} = R_{DOWN} \qquad Since \quad R_{UP} >> R_{DOWN}, \quad \left(\frac{R_{DOWN}}{R_{UP}}\right) \rightarrow 0 \quad (16)$$

2. Algorithm Used to Design the Heat Sinks

The main goal of this work is to design heat sinks for IMPATT sources to operate near *500 K* (Junction Temperature) during CW steady state operation. In Figure 7 the details of the algorithm used to design the heat sinks for IMPATT oscillators is described as a flow chart. At the first step, different input parameters (Thermal Conductivities, Thicknesses of different layers of the diode, ambient temperature, breakdown voltage, bias current density and efficiency) (Figure 7) are taken as input of the computer program. In the second step, the diode Thermal Resistance is found out using (5). Heat sink thickness (L_H) and Radius (R_H) are initialized in the third step. Next in the forth step, the Thermal resistance of the heat sink is determined. In fifth step, the Total Thermal Resistance (Diode-Heat sink combined) is determined using (16) and then in the sixth step the Junction Temperature is calculated. Now the calculated Junction

Temperature is checked whether it stays between *490 K* and *520 K* (seventh step).

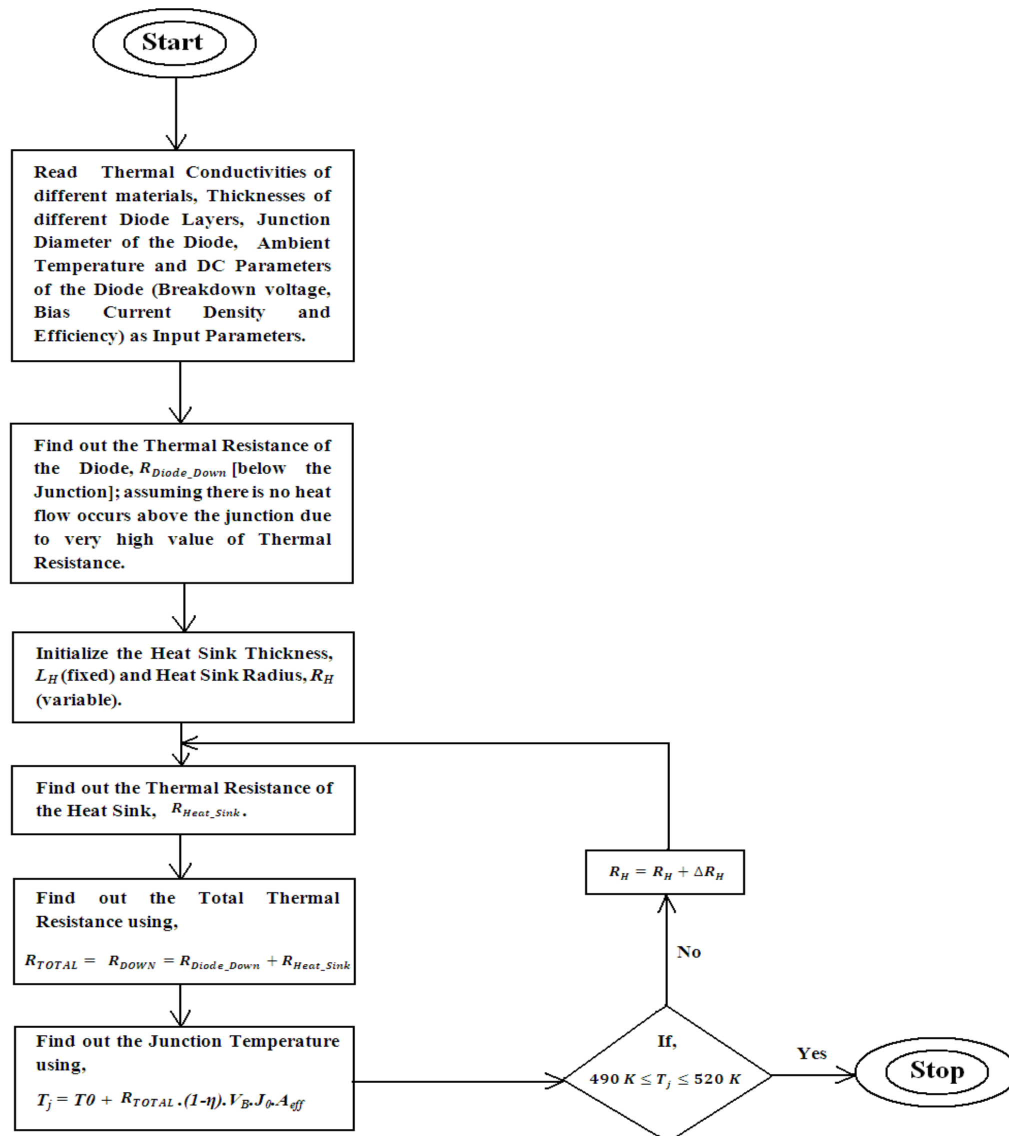

Figure 7: Flow Chart showing the Algorithm for Designing the Heat Sinks.

If yes then the computer program stops and gives the L_H and R_H values as designed values along with corresponding Total Thermal Resistance and Junction Temperature values; if no, then the control goes back to the fourth step with $R_H = R_H + \Delta R_H$ (with a small increment in Heat Sink Radius). In this way the program circulates in that loop until the condition told in seventh step is satisfied.

In the present work, for each case the heat sink thickness is kept fixed at some value and the heat sink radius is initialized at $R_H = 1\ \mu m$. R_H is increased by $\Delta R_H = 1\ \mu m$ in each iteration. ΔR_H is kept very small such that the checking condition ($490\ K \leq T_j \leq 520\ K$) attains easily.

3. Temperature Profile Inside the Heat Sink

Actual Structure of the Mesa Diode [Double Drift Region (DDR) IMPATT] is shown in Figure 8 [9]. During the steady state (CW-mode) operation actually the heat is generated at the p-n junction. This heat must be transferred to the ambience with a constant rate through heat sink to avoid the device burn out. Since the thickness of the diode is very small, it can be assumed that the junction temperature is equal to the diode heat sink interface temperature during steady state.

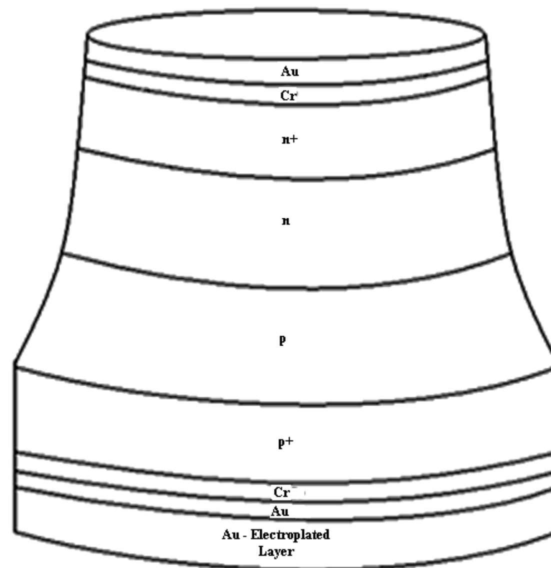

Figure 8: Mesa Structure of DDR IMPATT Diode.

Now the temperature distribution inside the semi-infinite heat sink will be found out. The temperature distribution within a homogeneous solid cylinder of isotropic media must satisfy Laplace Equation. Laplace equation in cylindrical co-ordirnate [2][6][7],

$$\nabla^2 T(r,z,\theta) = 0 \tag{17}$$

Due to symmetry, temperature is only the function of two spatial variables *r, z* only,

$$\frac{\partial^2 T(r,z)}{\partial r^2} + \frac{1}{r}\frac{\partial T(r,z)}{\partial r} + \frac{\partial^2 T(r,z)}{\partial z^2} = 0 \tag{18}$$

Equation (18) is satisfied by,

$$e^{-\lambda|z|} J_0(\lambda r) \tag{19}$$

For any λ, thus,

$$\int_0^\infty e^{-\lambda|z|} J_0(\lambda r) f(\lambda) d\lambda \tag{20}$$

Equation (20) will be solution of the problem, if $f(\lambda)$ can be chosen to satisfy the prescribed conditions in the plane $z = 0$. The two most interesting cases follow from the well known integrals involving the Bessel functions [6],

$$\int_0^\infty J_0(\lambda r) sin(\lambda R_0) \frac{d\lambda}{\lambda} = sin^{-1}\left(\frac{R_0}{r}\right) \qquad r > R_0$$
$$= \frac{\pi}{2} \qquad r \le R_0 \tag{21}$$

$$\int_0^\infty J_0(\lambda r) J_1(\lambda R_0) d\lambda = 0 \qquad r > R_0$$
$$= \frac{1}{2R_0} \qquad r = R_0 \tag{22}$$
$$= \frac{1}{R_0} \qquad r < R_0$$

Here heat is supplied over the circular area $0 \le r \le R_0$ in the plane $z = 0$. Since the diode thikness is very small, again it will be valid approximation that temperature distribution at the junction of the diode is almost same as at the diode heat sink interface [Temperature distribution at the interface is taken as uniform here] [4].

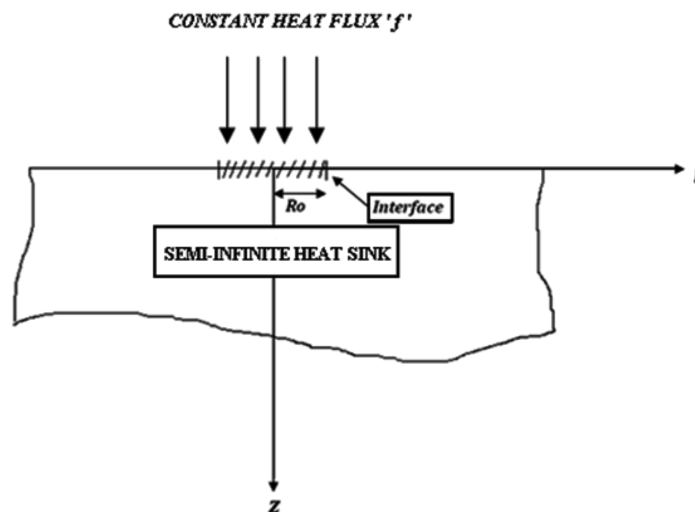

Figure 9: Figure illustrating the Mesa diode Semi-infinite heat sink interface.

The region $z > 0$ with constant flux *'f'* over the circular area $r \le R_0$ and zero over $r > R_0$. So, the boundary conditions will be,

Boundary Conditions:

$$\left.\frac{\partial T}{\partial z}\right|_{z=0} = -\frac{f}{k} \qquad 0 < r \le R_0$$
$$= 0 \qquad r > R_0 \tag{23}$$

Using (20), (22) & (23) we get [3][6],

$$T(r,z) = \frac{fR_0}{k}\int_0^{\infty} e^{-\lambda z} J_0(\lambda r) J_1(\lambda R_0)\frac{d\lambda}{\lambda} \tag{24}$$

A solution of (24) at the plane $z = 0$ is given by [3][10][11],

$$T(r,0) = \frac{fR_0}{k}\frac{2}{\pi}E\left(\frac{r}{R_0}\right) \qquad 0 < r < R_0 \tag{25}$$

$$T(r,0) = \frac{fR_0}{k}\frac{2}{\pi}\frac{r}{R_0}\left[E\left(\frac{R_0}{r}\right) - \left(1 - \left(\frac{R_0}{r}\right)^2\right)K\left(\frac{R_0}{r}\right)\right] \qquad R_0 < r < \infty \tag{26}$$

Where, $K(m)$ and $E(m)$ are the Complete Elliptic Integrals of the First & Second Kind respectively. Definitions of them are as following,

The Complete Elliptic Integral of First Kind is,

$$K(m) = F\left(\frac{\pi}{2}\middle| m\right) \tag{27}$$

Where, F is the Elliptic Integral of First Kind,

$$K(m) = \int_0^1 \left[(1-t^2)(1-mt^2)\right]^{-\frac{1}{2}} dt = \int_0^{\frac{\pi}{2}} \left[(1 - m\sin^2\theta)\right]^{-\frac{1}{2}} d\theta \tag{28}$$

The Complete Elliptic Integral of Second Kind is,

$$E(m) = E(K(m)) = E\left(\frac{\pi}{2}\middle| m\right) \tag{29}$$

Where,

$$E(m) = \int_0^1 \left[(1-t^2)^{-\frac{1}{2}}(1-mt^2)^{\frac{1}{2}}\right] dt = \int_0^{\frac{\pi}{2}} \left[(1 - m\sin^2\theta)\right]^{\frac{1}{2}} d\theta \tag{30}$$

Some definitions of K and E use the Modulus k instead of the parameter m. They are related by,

$$k^2 = m = \sin^2\alpha \tag{31}$$

The actual temperature is $\frac{fR_0}{k}$ times the normalized temperature, where 'f' is the power input density to the heat sink, R_0 is the diode radius at the interface, k is Thermal Conductivity of Heat

Sink material. The improper integral of (8) is evaluated by numerical method. Detail of the evaluation procedure of the integral is given in Appendix A.

RESULTS AND DISCUSSION

A double iterative field maximum computer method has been developed (by the authors) which solves the basic device equations (e.g. Poisons Equation, Current Density Equations and Current Continuity Equations) simultaneously, considering the mobile space charge effect. This computer program is used to design CW DDR IMPATT diodes with different base materials and optimized those performances to properly operate at 94 GHz. Structural and simulated DC parameters of those designed diodes are listed in TABLE I.

Table I: Diode Structural and Simulated Dc Parameters

BASE MATERIAL AND DIODE STRUCTURE	FREQUENCY OF OPERATION	*p*-EPITAXIAL LAYER THICNESS (μm)	*n*-EPITAXIAL LAYER THICNESS (μm)	BIAS CURRENT DENSITY (Amp/m^2)	BREAKDOWN VOLTAGE (*Volt*)	EFFICIENCY (%)
Si- DDR	94 GHz	0.300	0.400	6.00×10^8	21.98	10.07
InP- DDR	94 GHz	0.352	0.350	1.10×10^8	27.50	16.30
4H-SiC- DDR	94 GHz	0.555	0.550	1.80×10^8	207.60	16.30

In this paper, the main aim is to determine the Thermal Resistances of the diodes. To do this, the thicknesses of the all layers of the diode must be known exactly. Thicknesses of the epitaxial layers are already available from TABLE I for each diode. So the thicknesses of p^+ and contact-layers on p^+ -layer must also be known (as we are interested only on the Thermal Resistances of the diodes below the junction). For the Si-DDR, p^+-layer thickness is taken as *500 nm* and it is coated with a *Cr*-layer about *60 nm* which is followed by an evaporated *Au*-layer of *300 nm*. The coating is done by e-beam evaporation of metals on Si wafer having appropriate doping profile. Substrate heating is required for good adhesion of metal layers. Finally a *5000 nm Au*-layer is electroplated on evaporated *Au*-layer. In case of InP-DDR, the thicknesses of the p^+-layers are taken as *500 nm*. In this diode metallization is done in the same process as in case of Si-DDR discussed previously (thicknesses of the contact layers are also same). In case of 4H-SiC-DDR, at first metallization is done by *Al/Ti/Al* layers respectively with thicknesses *40 nm/20 nm/40 nm* over the p^+ -layer (*900 nm*). Next on the last *Al* coating *Ti/Au* are evaporated (*60 nm/ 300 nm*) respectively. Lastly a *5000 nm Au*-layer is electroplated on evaporated *Au*-layer.

Another two important things to determine the Thermal Resistances of the diodes are (1) Diameters of the diode junctions ($2r_0$) and Diameters of the diodes at diode-heat sink interface ($2r_{n-1}$) and (2) Thermal Conductivities (k) of the all layers. For continuous wave (CW) operation normally junction diameter is, $2r_0 = 35\ \mu m$ and diameter of the diodes at diode-heat sink interface is, $2r_{n-1} = 200\ \mu m$. And the thermal conductivities (at *500 K*) of all the materials (diode base materials, contact materials and heat sink materials) are given in tabular form in TABLE II. Also for determining the thermal resistances of *p*-layers of the diodes value of *n* [Figure 5] is taken as *100*, which is a sufficient approximation for this order of dimensions.

Table II: Thermal Condutivities of Different Materials At *500 K*

MATERIALS	BASE MATERIALS			CONTACT MATERIALS						HEAT SINK MATERIALS	
	Si	InP	4H-SiC	Au	Ni	Ti	Cr	Al	Pd	Cu	Type-IIA Diamond
THERMAL CONDUCTIVITY [Watt/m^{o}C]	80	68	370	317	90.7	21.9	93.7	237	71.8	396	1200

Both metallic (copper) and type-IIA diamond are conventionally used as heat sink materials. However a significant thermal advantage is gained by using type-IIA diamond heat sinking. At first to compare the total thermal resistances of all diodes (TABLE I), heat sink made of copper and diamond of same dimensions (Heat Sink Radius, $R_H = 500\ \mu m$ and Thickness, $L_H = 3000\ \mu m$) is considered. The total thermal resistances of each diode are plotted as a function of diode diameter (for both copper and diamond of same dimensions). A good comparison can be obtained from this graph (Figure 10). Depending on the thicknesses and thermal conductivities of different layers of the diodes total thermal resistances attained different values for a particular diode diameter. From Figure 10, it is cleared that at the diode diameter of our interest (i.e. $2r_0 = 35\ \mu m$) total thermal resistance of Si-DDR (94 GHz) attains the highest value (about *11.09 ^{o}C/Watt for copper heat sink and 4.63 ^{o}C/Watt for diamond heat sink*) and 4H-SiC-DDR (94 GHz) attains the lowest value (about *10.09 ^{o}C/Watt for copper heat sink and 3.63 ^{o}C/Watt for diamond heat sink*). Due to very small thermal conductivity (80 Watt/m^{o}C at 500 K) of Si, Si-DDR (94 GHz) diode attains such larger value of total thermal resistance; and due to very large value of thermal conductivity of (370 Watt/m^{o}C at 500 K) 4H-SiC, 4H-SiC-DDR (94 GHz) attains such smaller total thermal resistance despite its thickest *p*-layer. For a diode diameter *35 μm* of, the value of total thermal resistance for diamond is roughly *58%* of the corresponding value of the copper. Thus for a fixed output power and efficiency, the temperature rise over ambient for diamond heat sinking is only *58%* of the corresponding rise for copper. Conversely, for a fixed junction temperature and efficiency, the output power [$P_{RF} = (\Delta T/R_{TOTAL})(\eta/1-\eta)$, $\Delta T = T_j - T_0$] can be increased about *72%* by using diamond rather than copper [5]. However, efficiency is also enhanced with diamond heat sinking so that the actual power increase can be even greater [1].

Table III: Heat Sink Dimensions, Thermal Resistance And Junction Temperature

BASE MATERIAL AND DIODE STRUCTURE	HEAT SINK DIMENSIONS				THERMAL RESISTANCE (*^{o}C/Watt*)		JUNCTION TEMPERATURE (*K*)	
	COPPER		DIAMOND		USING COPPER HEAT SINK	USING DIAMOND HEAT SINK	USING COPPER HEAT SINK	USING DIAMOND HEAT SINK
	DIAMETER (*μm*)	THICKNESS (*μm*)	DIAMETER (*μm*)	THICKNESS (*μm*)				
Si- DDR	620	2000	360	2000	18.23	17.88	508	504
InP- DDR	440	5000	260	5000	84.35	79.80	505	494
4H-SiC-DDR	860	1400	500	1400	6.55	6.40	497	493

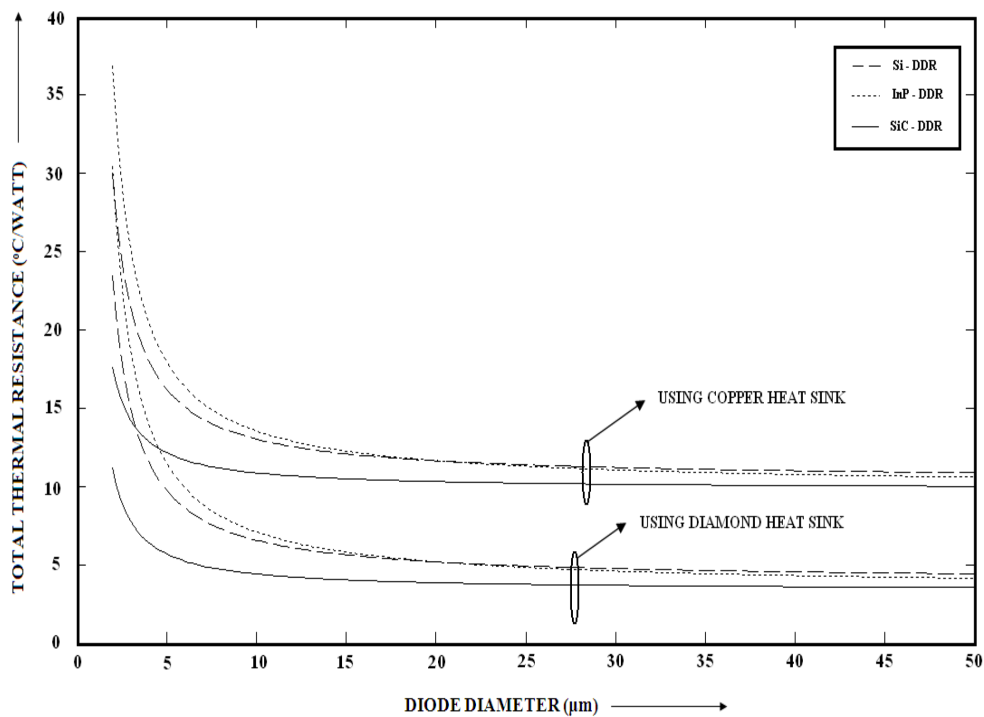

Figure 10: Total Thermal Resistance as a function of Diode Diameter for fixed values of the Heat Sink dimensions [Heat Sink Radius, $R_H = 500\ \mu m$ and Thickness, $L_H = 3000\ \mu m$].

Now the heat sinks are designed for each diode using both copper and diamond to operate those in CW steady state condition near *500 K* junction temperature using the algorithm described in Section III. The designed heat sink dimensions, calculated total thermal resistances and corresponding junction temperatures are listed in TABLE III. Form the TABLE III, it is evident that the total thermal resistance of InP-DDR (94 GHz) is largest and 4H-SiC-DDR (94 GHz) is smallest. These can be explained from TABLE I. From TABLE I, it is clear that the dissipated power [$P_{dissipated} = (1-\eta).V_B.J_0.A_{eff}$; *where* V_B = *Breakdown voltage,* J_0 = *Bias current density,* A_{eff} = *Effective junction area*] is smallest for InP-DDR (94 GHz) and largest for 4H-SiC-DDR (94 GHz). Eventually, to keep almost same junction temperature [$T_j = T_0 + R_{TOTAL}.\ P_{dissipated}$] near *500 K* the total thermal resistance [R_{TOTAL}] must be largest for InP-DDR (94 GHz) and smallest for 4H-SiC-DDR (94 GHz). So, to make R_{TOTAL} largest heat sink radius values [diamond and copper heat sinks] must be smallest [$R_{th} \infty 1/r^2$]; similarly to make R_{TOTAL} smallest heat sink radius values [diamond and copper heat sinks] must be largest. That is way it can be seen that, the radius values of both diamond and copper heat sinks are smallest for InP-DDR (94 GHz) [smallest heat sink volume] and largest for 4H-SiC-DDR (94 GHz) [largest heat sink volume].

The algorithm used here (described in Section III) only adjusts the heat sink radius values, keeping the heat sink thickness values fixed to obtain the equivalent junction temperature [near *500 K*] during CW steady state operation for a particular diode [for both copper and diamond

heat sinks]. In Figure 11 junction temperatures of all the diodes as a function of the total thermal resistance is plotted.

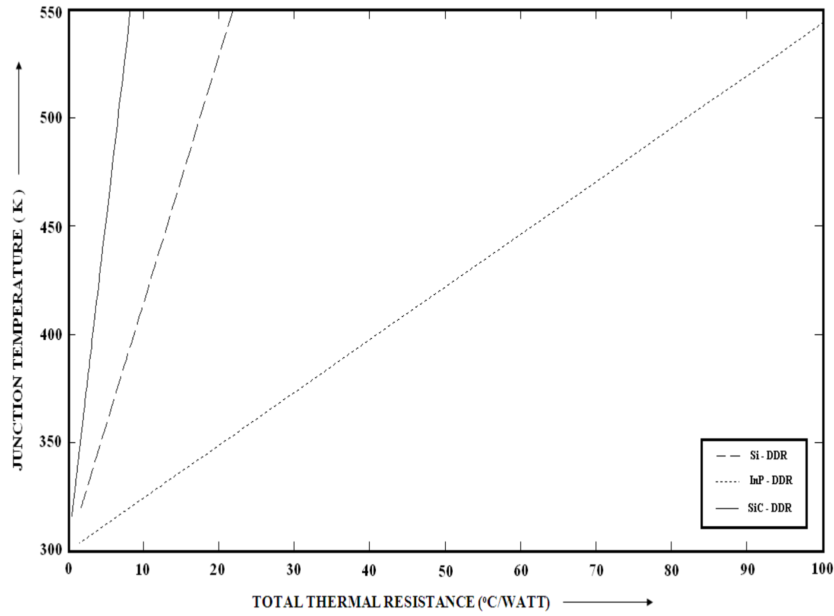

Figure 11: Junction Temperature as a function of Total Thermal Resistance.

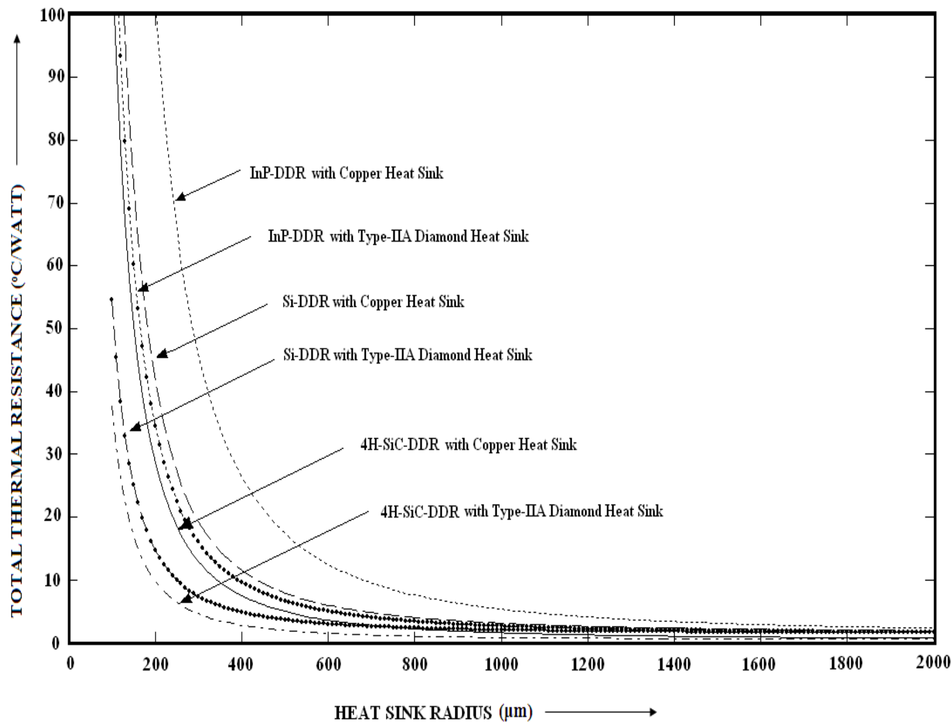

Figure 12: Total Thermal Resistance as a function of Heat Sink Radius [copper and diamond heat sink thicknesses are kept same for a particular diode].

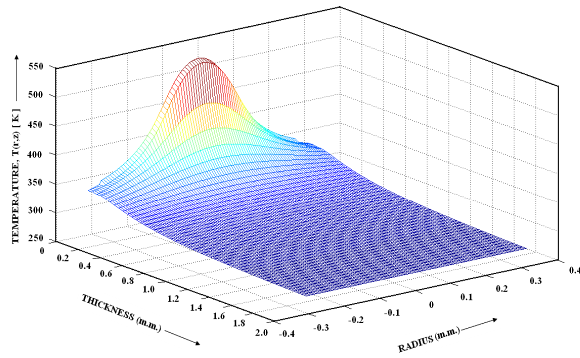

(a)

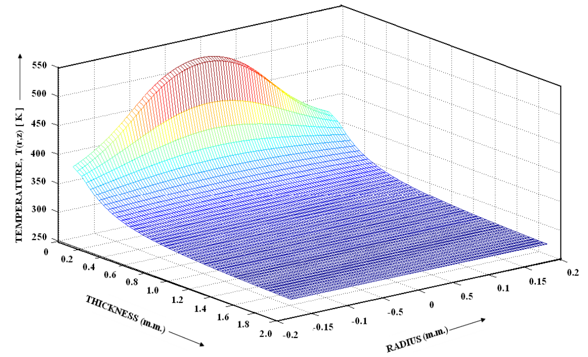

(b)

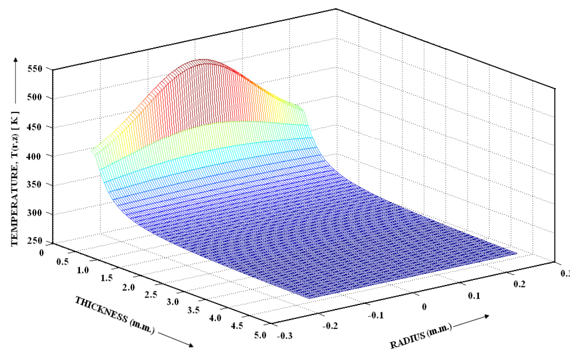

(c)

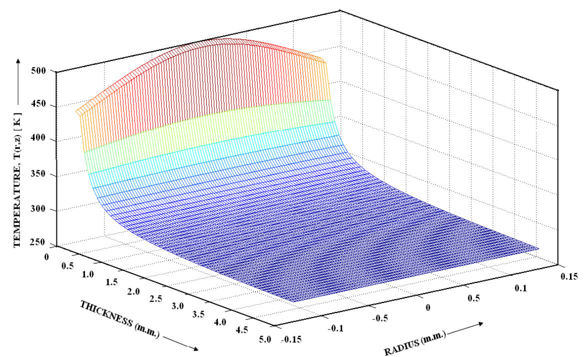

(d)

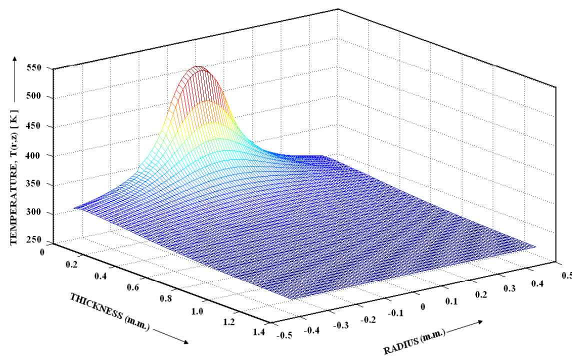

(e)

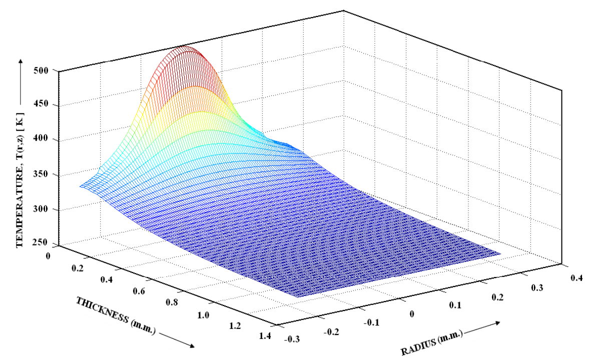

(f)

Figure 13: Temperature as a function of radius and thickness of the heat sink; (a) Si-DDR with copper heat sink, (b) Si-DDR with type-IIA diamond heat sink, (c) InP-DDR with copper heat sink, (d) InP-DDR with type-IIA diamond heat sink, (e) 4H-SiC-DDR with copper heat sink, (f) 4H-SiC -DDR with type-IIA diamond heat sink.

The value of R_{TOTAL} required to obtain T_j near *500 K* for a particular diode can be obtained from the corresponding Junction Temperature vs Total Thermal Resistance graph. After getting required R_{TOTAL} values for a particular diode the corresponding heat sink radius values (copper and diamond heat sink thicknesses are kept same for a particular diode) can be obtained from Figure 12 (Total Thermal Resistance vs Heat Sink Radius plot). From Figure 12 it can be observed that the total thermal resistances become almost equal for very large values of R_H (for fixed thickness, L_H); because for very large values of R_H the dependence of the Thermal Resistance of the heat sink becomes almost independent of the heat sink material thermal conductivity (k_H). So, it can be concluded that, for very large values of R_H (for fixed thickness, L_H) diamond and copper heat sinks will give the same performance.

During the steady state (CW) operation of the IMPATT oscillator the heat generated at the p-n junction of the diode must be transferred to the ambience with a very high rate. To achieve this purpose heat sink made of some special materials having very high thermal conductivities [e.g. copper or diamond (type-IIA)] has to be attached below the diode. Heat sink dimensions must be chosen such that at the end surface of the heat sink temperature falls to ambient temperature during steady state. For CW operation of the IMPATT oscillator the diode heat sink interface radius is taken as *100µm*. The evaluation procedure of (24) is available from Appendix A. Using this (24) authors have plotted Temperature Distribution inside the *Copper* and *Diamond Semi infinite Heat Sinks* as a function of *r* and *z* for all the diodes as shown in Figure 13 [11]. Temperature distributions inside the heat sinks actually depends on the dimensions of heat sinks, heat sink materials and the diode-heat sink interface temperature. Here it can be assumed that the junction temperature of a diode is approximately equal to the diode-heat sink interface temperature. As the thickness of a diode below the junction is much smaller compared to the heat sink thickness, the thermal resistance of that portion (R_{Diode_Down}) is very small. That is why very less amount of temperature fall occurs from the junction to the diode-heat sink interface.

CONCLUSION

Formulation of total thermal resistance for ordinary mesa structure IMPATT diode mounted on semi-infinite heat sink is presented in this paper. Accuracy in determination of total thermal resistances actually provides accurate and optimum design of heat sinks for steady and safe operation of IMPATT oscillators in continuous wave mode which is capable of avoiding burn-out phenomena. Keeping in mind the cost of the whole system, typical equivalent heat sink designs are presented in this paper for IMPATT diode sources with different base materials operating at different frequencies by using both diamond [High Cost] and copper [Comparatively Low Cost]. In this paper analytical approach to solve the Laplace Equation to obtain the temperature distribution inside the semi-infinite heat sink during steady state (CW) operation of IMPATT oscillator is also presented. Temperature distributions for typical copper and diamond heat sinks are also plotted graphically to visualize the actual fact. This approach is very much useful to design heat sinks for CW IMPATT oscillators. It can be easily observed that as the thermal conductivity of diamond is almost three times larger than that of copper near *500 K*, i.e. why required diamond heat sink is much smaller in size than copper heat sink for equivalent operation.

APPENDIX A

Evaluation of Integral of (24) applying Numerical Method: The improper integral of (24) can be evaluated by following way using Numerical Method [Simpson's 1/3 - Rule].

$$I = \int_0^\infty e^{-\lambda z} J_0(\lambda r) J_1(\lambda R_0) \frac{d\lambda}{\lambda} \tag{A1}$$

Put, $e^{-\lambda z} = x$ $\left[\lambda = -\frac{1}{z} ln(x) = \frac{1}{z} ln\left(\frac{1}{x}\right)\right]$

$$\Rightarrow e^{-\lambda z} d\lambda = -\frac{dx}{z}$$

λ	0	∞
x	1	0

After changing variable (A1) becomes,

$$I = -\int_1^0 \frac{J_0\left(\frac{r}{z} ln\left(\frac{1}{x}\right)\right) J_1\left(\frac{R_0}{z} ln\left(\frac{1}{x}\right)\right)}{ln\left(\frac{1}{x}\right)} dx = \int_0^1 \frac{J_0\left(\frac{r}{z} ln\left(\frac{1}{x}\right)\right) J_1\left(\frac{R_0}{z} ln\left(\frac{1}{x}\right)\right)}{ln\left(\frac{1}{x}\right)} dx \tag{A2}$$

Here one can see that the integrant is undefined at $x = 1$ & $x = 0$. To avoid these discontinuities it can be assumed that the lower limit as $x = 0.000001$ & upper limit as $x = 0.999999$ with maintaining sufficient accuracy.

$$I = \int_{0.000001}^{0.999999} \frac{J_0\left(\frac{r}{z} ln\left(\frac{1}{x}\right)\right) J_1\left(\frac{R_0}{z} ln\left(\frac{1}{x}\right)\right)}{ln\left(\frac{1}{x}\right)} dx \tag{A3}$$

Now Numerical technique can be used to find out the integration of above (18). Here Simpson's 1/3 – Rule is used. According to this Rule,

$$\int_{x_0}^{x_n} y.dx = \frac{h}{3}\left[y_0 + 4(y_1 + y_3 + y_5 + \dots\dots\dots + y_{n-1}) + 2(y_2 + y_4 + y_6 + \dots\dots\dots + y_{n-2}) + y_n\right] \tag{A4}$$

Where, $x_n = x_0 + nh$, $n = 999998$, $x_n = 0.999999$, $x_0 = 0.000001$ and $h = 0.000001$.

Integrant, $$y = \frac{J_0\left(\frac{r}{z} ln\left(\frac{1}{x}\right)\right) J_1\left(\frac{R_0}{z} ln\left(\frac{1}{x}\right)\right)}{ln\left(\frac{1}{x}\right)} \tag{A5}$$

Evaluation of the Integration has been carried out by using MATLAB software.

REFERENCES

[1] T. A. Midford, R. L. Bernick, *IEEE Trans. on MTT*, **1979**, vol. MTT-27, no. 5, pp. 483-492.
[2] D. P. Kennedy D, *J. Appl. Phys.*, **1960**, vol. 31, p. 1490.
[3] J. Frey, *IEEE Trans. Electron Devices*, **1972**, vol. ED-19, p. 981.
[4] R. L. Bernick, *Electronic Letters*, **1972**, vol. 8, no. 7, p. 180.
[5] J. V. DrLorenzo, W. C. Niehaus, J. R. Velebir, D. E. Iglesias, *IEEE Trans. Electron Devices*, **1975**, vol. ED-22, no. 8, pp. 509-514.
[6] H. S. Carslaw, J. C. Jaeger, Conduction of Heat in Solids, Oxford: Clarendon, **1959**.

[7] J. P. Holman, Heat Transfer, Tata McGraw Hill [Ninth Edition].
[8] G. Gibbons, T. Misawa, *Solid State Electron.*, **1968**, vol. 11, p. 1007.
[9] B. Pal, A. Acharyya, A. Das, J. P. Banerjee, *Proceedings of National Conference on MDCCT 2010, Burdwan*, **2010**, p. 58-59.
[10] A. Acharyya, B. Pal, J. P. Banerjee, *International Journal of Electronic Engineering Research*, **2010**, vol 2, no. 4, pp. 553-567.
[11] A. Acharyya, B. Pal, J. P. Banerjee, *International Journal of Engineering Science and Technology*, **2010**, vol. 2, no. 10, pp. 5142-5149.